



# A narrow range multielectrochromism from 2,5-di-(2-thienyl)-1H-pyrrole polymer bearing pendant perylenediimide moiety



Emre Sefer<sup>a</sup>, Hakan Bilgili<sup>b</sup>, Burak Gultekin<sup>b</sup>, Murat Tonga<sup>c</sup>, Sermet Koyuncu<sup>d,\*</sup>

<sup>a</sup> Department of Chemistry, Faculty of Sciences and Arts, Çanakkale Onsekiz Mart University, 17020, Çanakkale, Turkey

<sup>b</sup> Solar Energy Institute, Ege University, Bornova, 35100, Izmir, Turkey

<sup>c</sup> Department of Chemistry, University of Massachusetts-Amherst, Amherst, MA, 01003, USA

<sup>d</sup> Department of Chemical Engineering, Faculty of Engineering, Çanakkale Onsekiz Mart University, 17020, Çanakkale, Turkey

## ARTICLE INFO

### Article history:

Received 19 June 2014

Received in revised form

21 July 2014

Accepted 4 August 2014

Available online 14 August 2014

Dedicated to Professor Eyup Ozdemir.<sup>1</sup>

### Keywords:

Conjugated polymers

Donor–acceptor polymers

Electrochromic materials

Photoinduced electron transfer

Perylenediimides

2,5-di-(2-thienyl)-1H-pyrrole

## ABSTRACT

A new 2,5-di-(2-thienyl)-1H-pyrrole (SNS) moiety containing perylenediimide (PDI) acceptor as pendant side chain has been synthesized for an electroactive monomer and then directly deposited onto ITO/glass surface via electrochemical polymerization process. The observed electronic interaction only at the excited state due to the presence of phenylene spacer between SNS-donor and PDI-acceptor moiety leads to efficient fluorescence quenching. This charge separation behavior was also proved by theoretical DFT calculations. Thin films of the polymer electropolymerized onto transparent electrode exhibited ambipolar multi-electrochromic behavior including purple, violet-red-khaki-blue colors in both anodic and cathodic regime only between  $-1.2$  and  $1.0$  V. We further demonstrated that this polymer film has a high contrast ratio ( $\Delta T = 45\%$  at  $900$  nm), a faster response ( $0.5$  s), high coloration efficiency ( $254$  cm<sup>2</sup> C<sup>-1</sup>) and retained its performance by 92% even after 5000 cycles.

© 2014 Elsevier Ltd. All rights reserved.

## 1. Introduction

Since polyacetylene as first conducting polymer was announced by Shirakawa and co-workers in 1977 [1], these polymers have received much attention in the field of science and technology [2]. These polymers have various application areas such as light emitting diodes (LEDs) [3–6], organic photovoltaics (OPV) [7–9], organic transistors (OFETs) [10,11], displays [12], smart windows [13] and camouflage materials [14]. Construction of conjugated polymers containing multiple redox-active chromophores is important for the preparation of new polymeric optoelectronic materials, which exhibit various low redox states derived from distinct absorption bands at different wavelengths, depending on the structure of the material [15,16]. In the literature, lots of building blocks have been used to obtain conjugated polymers with different optical, electrochemical and physical properties. It is essential to achieve electroactive polymers with band gaps as low

as 0.3–0.5 eV which results from alternating electron donor and electron-accepter units combined through  $\pi$ -conjugation with intrinsic intramolecular charge transfer (ICT) character. Thus, this methodology offers an effective way to reduce the band gap of resultant polymers by the incorporation of building segments with a higher HOMO and a lower LUMO level [17,18]. Electroactive polymers are also suitable for use in electrochromic materials because of not only their structurally controlled energy band gap but also easy color tunability, processibility, high contrast ability and a fast response time [19–24]. Furthermore, electrochromic polymers can exhibit electrochemical stability upon continuous redox switching between their various colored states without any noticeable decline in performance, so they have been considered excellent candidates for the practicality of electrochromic devices [15–26].

On the other hand, recently reported materials, 2,5-di-(2-thienyl)-1H-pyrrole (SNS) derivatives [27,28], have outstanding properties for electrochromic applications such as (i) the oxidation potential of the SNS derivatives is lower (about  $+0.7$  V vs. SCE) than those of many of other electroactive materials, (ii) Paal–Knorr synthesis offers easy attachment of side chains into the main monomer, (iii) providing good quality of the films of poly-SNS

\* Corresponding author. Tel.: +90 286 2180541; fax: +90 286 2180540.

E-mail addresses: [skoyuncu@comu.edu.tr](mailto:skoyuncu@comu.edu.tr), [sermetkoyuncu@hotmail.com](mailto:sermetkoyuncu@hotmail.com) (S. Koyuncu).

<sup>1</sup> Deceased March 25, 2014.

which can be easily generated onto ITO/glass surface, and thus can yield a high performance [26]. Moreover, the introduction of an electroactive or a photoactive moiety into SNS backbone can provide the band gap tunability and valuable properties. On the other hand, perylene diimides (PDIs) represent a class of highly stable n-type semiconductors with relatively high electron affinity and excellent charge transport property [29]. There has been an increasing interest in the incorporation of PDIs as energy- or electron-acceptors. PDIs have been inserted between donor and acceptor segments in conjugated oligomeric or polymeric building blocks in order to avoid extensive clustering and macro phase separation of the donor and acceptor phases, which may occur in case of blending the two separate components [30,31]. PDI exhibits an efficient charge separation in the solution and solid state. Due to the favorable interactions of the donor parts with acceptor parts in the solid state, these polymers result in the formation of alternating SNS and PDI assemblies [32,33].

In this paper, we present a new SNS based electroactive monomer bearing PDI with a branched alkyl chain as acceptor subunit. Remarkable fluorescence quenching in the PDI core was observed due to efficient intramolecular electron transfer from SNS-donor to PDI-acceptor at the excited state. The polymer film was obtained onto ITO/glass surface by electrochemical process. Owing to dual redox behavior in low driving potential, the polymeric film exhibits a wide range of colors including purple, violet-red-khaki-blue in both anodic and cathodic regime. Therefore, the generation of an attractive palette of colors in a narrow range of  $-1.2$ – $1.0$  V makes these polymers promising candidate for electrochromic devices.

## 2. Experimental

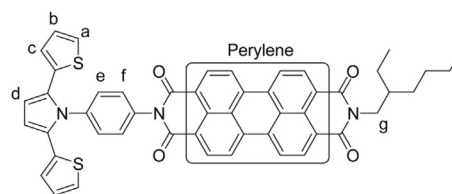
### 2.1. Materials

All materials were supplied from Aldrich, Merck and Fluka, and were used without further purification. The syntheses and characterizations of 1,4-Bis(2-thienyl)butan-1,4-dione [34], 1-(4-nitrophenyl)-2,5-di(thiophen-2-yl)-1H-pyrrole [35], 4-(2,5-di(thiophen-2-yl)-1H-pyrrol-1-yl)aniline [36], N,N-di(2-ethylhexyl)perylene-3,4,9,10-tetracarboxylic acid diimide [37], N-(2-Ethylhexyl)-3,4,9,10-perylenetetracarboxylic acid 3,4-anhydride-9,10-imide [37] were previously described in the literature.

### 2.2. Synthesis of SNS-PDI

N-(2-Ethylhexyl)-3,4,9,10-perylenetetracarboxylic acid 3,4-anhydride-9,10-imide (0.533 g, 1.92 mmol), was added into 40 mL dry pyridine and refluxed under argon atmosphere for 30 min. Then, 4-(2,5-di-2-thienyl-1H-pyrrole-1-yl)aniline[4-(2,5-di-2-thienyl-1H-pyrrole-1-yl)phenyl]amine (0.155 g, 0.481 mmol) was added in small portions and this mixture was stirred at  $120$  °C for 8 h. Then, the reaction mixture was cooled to room temperature and poured into HCl solution (3 M, 500 mL). The resulting precipitate (1.11 g) was collected by filtration, washed with  $\text{NaHCO}_3$  solution (100 mL) and water (50 mL), and then the product was purified by column chromatography (silica gel, 3/1;  $\text{CHCl}_3$ /hexane). The pure product dried at  $80$  °C in vacuum oven. Yield: 89% 0.25 g.

FT-IR ( $\text{cm}^{-1}$ ): 3036, 3012 (C–H, aromatic); 2922, 2851 (C–H aliphatic); 1697, 1656 (C=O imide); 1573, 1563 (C=C aromatic).  $^1\text{H-NMR}$  ( $\text{CHCl}_3$ -d):  $\delta$  ppm, 8.64 (d, 4H, C–H perylene); 8.52 (d, 4H, perylene); 8.10 (d, 2H, H<sub>f</sub>), 7.91 (d, 2H, H<sub>a</sub>), 7.62 (d, 2H, H<sub>e</sub>); 7.43 (d, 2H, H<sub>c</sub>); 7.32 (m, 2H, H<sub>b</sub>); 6.84 (s, 2H, H<sub>d</sub>); 4.32 (m, 2H, N–CH<sub>2</sub>); 1.51–0.83 (m, 15H, C–H aliphatic), MALDI-ToF ( $m/z$ ): [ $M^+$ ] calcd. for  $\text{C}_{50}\text{H}_{39}\text{N}_3\text{O}_4\text{S}_2$ , 809.99; found, 809.92.



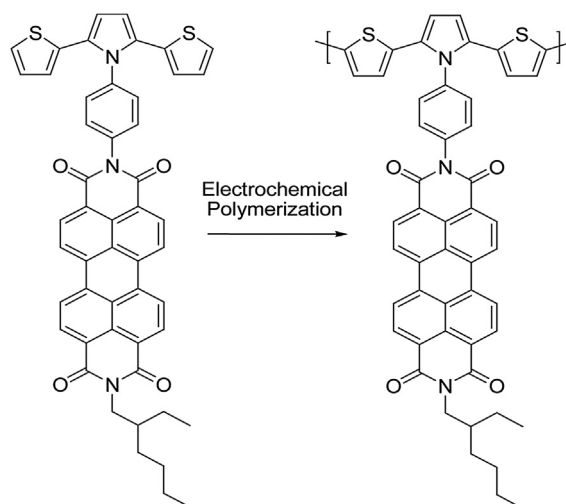
### 2.3. Electrochemical polymerization of SNS-PDI

Electrochemical polymerization processes were carried out in a dichloromethane solution of  $2.0 \times 10^{-3}$  M SNS-PDI monomer and 0.1 M TBAPF<sub>6</sub> by repetitive cycling between 0 and 1.0 V at a scan rate of  $100 \text{ mV s}^{-1}$ . A platinum wire was used as a counter electrode and Ag wire as a reference electrode. The polymer was directly deposited onto platinum disk ( $0.02 \text{ cm}^2$ ) or ITO/glass surface ( $8$ – $12 \Omega$ ,  $0.8 \times 5 \text{ cm}^2$ , active area adjusted to  $1 \text{ cm}^2$ ). After deposition of poly-SNS-PDI, the ITO/glass surface was washed with acetonitrile to remove the impurities and oligomeric by-products in electrolyte (Scheme 1).

### 2.4. Instrumentation

FT-IR spectra were recorded by a Perkin Elmer FT-IR Spectrum One by using ATR system ( $4000$ – $650 \text{ cm}^{-1}$ ).  $^1\text{H NMR}$  (Bruker Avance DPX-400) data were recorded at  $25$  °C by using  $\text{CHCl}_3$ -d as solvent and TMS as internal standard.

Cyclic voltammetry (CV) technique used for electrochemical measurements were performed by Biologic SP-50 electrochemical workstation. These measurements were carried out under argon atmosphere and the electrochemical cell includes an Ag wire as reference electrode (RE), Pt wire as counter electrode and glassy Pt disk as working electrode (WE) immersed in supporting electrolyte solution in consist of  $2.0 \times 10^{-3}$  M SNS-PDI monomer and 0.1 M TBAPF<sub>6</sub> in dichloromethane. HOMO and LUMO energy levels of SNS-PDI and corresponding polymer were calculated according to the inner reference ferrocene redox couple  $E^\circ(\text{Fc}/\text{Fc}^+)_{\text{on}} = +0.38 \text{ V}$  (vs. Ag wire; see Supplementary data, Fig. S8) by using the equation  $E_{\text{HOMO/LUMO}} = -e(E_{\text{ox/red}} - E_{\text{Fc}}) + (-4.8 \text{ eV})$  [38]. Onset values of oxidation/reduction potentials were taken into account while calculating HOMO/LUMO energy levels. UV–Vis absorption spectra were measured by Analytic Jena Speedcord S-600 diode-array



**Scheme 1.** Electrochemical polymerization reaction of SNS-PDI.

spectrophotometer. The optical band gap ( $E_g$ ) of products was calculated from their absorption edges by using this formula  $E_g(\text{eV}) = 1241/\lambda_{\text{on}}$  [39]. Frontier molecular orbitals have been studied by DFT calculations with Spartan10 program at the parameters of B3LYP and 6-31G\*\* basis set.

Spectro-electrochemical measurements were carried out to evaluate absorption spectra of these polymer films under applied potential [40]. The spectro-electrochemical cell consists of Ag wire (RE), Pt wire (CE) and ITO/glass as transparent working electrode (WE) in a quartz cell. All measurements were carried out in the 0.1 M TBAPF<sub>6</sub> as supporting electrolyte in acetonitrile. Colorimetry measurements were performed by using an Analytic Jena Specord S600 UV–Vis spectrophotometer, which contains a chromameter module (standard illuminator D65, field of with 10° observer) with viewing geometry as recommended by “International Commission on Illumination” (CIE) [41]. According to the CIE system, the color is consist of three attributes; luminance (L), hue (a), and saturation (b). Platinum cobalt DIN ISO 621, iodine DIN EN 1557, and Gardner DIN ISO 6430 are the references of colorimetric measurement. These parameters were applied for the neutral, oxidized and reduced states of poly-SNS-PDI deposited onto ITO/glass surface.

### 3. Results and discussion

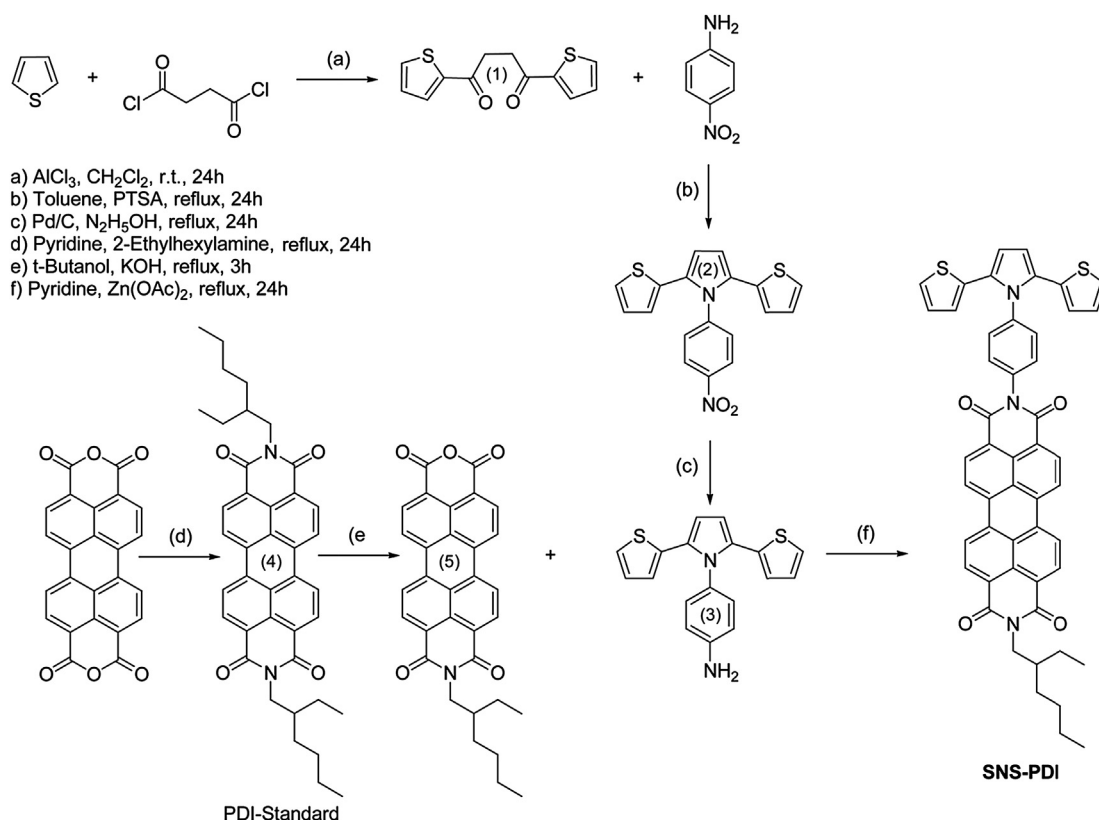
#### 3.1. Synthesis and characterization

A novel electroactive SNS monomer containing PDI subunit was synthesized in six steps (Scheme 2). The SNS containing nitro subunit, 1-(4-nitrophenyl)-2,5-di(thiophen-2-yl)-1H-pyrrole (**2**) [35], was synthesized via Paal–Knorr reaction with 1,4-Bis(2-thienyl)butan-1,4-dione [34] and 1-amino-4-nitrobenzene in presence of p-toluenesulfonic acid (PTSA) as catalyst by using

toluene as solvent. The nitro compound, **2**, was reduced to 4-(2,5-di(thiophen-2-yl)-1H-pyrrol-1-yl)aniline by using Pd on activated charcoal (Pd/C) and hydrazinium hydroxide (N<sub>2</sub>H<sub>5</sub>OH) (**3**) [36]. Meanwhile, N,N-di(2-ethylhexyl)perylene-3,4,9,10-tetracarboxylic acid dimide [37], N-(2-Ethylhexyl)-3,4,9,10-perylenetetracarboxylic acid 3,4-anhydride-9,10-imide (**5**) were synthesized and fully characterized according to the previously reported study [37]. The final product, **SNS-PDI**, was obtained by the condensation reaction between **3** and **5** with a yield of 81%.

Structures of all compounds were also fully identified by using FT-IR and <sup>1</sup>H NMR spectra. Significant changes were observed between the spectral properties of the initial compounds and SNS-PDI product. The characteristic signals arising from the amine group (–NH<sub>2</sub>) in **3** and anhydride carbonyl (O=C=O) in **5** disappeared in FT-IR spectrum of SNS-PDI product. Furthermore, characteristic strong imide (N–C=O) peaks at 1697–1656 cm<sup>−1</sup> appeared by the formation of SNS-PDI after the completion of final condensation reaction. In the <sup>1</sup>H NMR spectrum of **SNS-PDI**, doublet–doublet signals at 8.64–8.52 ppm are arising from the perylenediimide protons as expected. The singlet signal observed at 6.84 ppm is attributed to the protons on the pyrrole unit of SNS moiety. Besides, doublet signals at 8.10 and 7.62 ppm belonging to phenylene bridge between SNS-donor and PDI-acceptor moieties are the strongest evidence for the formation of the final product (see Supplementary data Fig. S1–7).

Potentiodynamic electrochemical polymerization of **SNS-PDI** carried out repetitive cycling at a potential between 0 and 1.0 V exhibited a new redox couple at 0.49–0.59 V ( $E_{p,1/2}^{\text{ox}} = 0.54\text{V}$ ). The increased current density after each successive cycle clearly indicated the formation and deposition of poly-SNS-PDI onto the surface of the WE (Fig. 1). The polymer film onto ITO/glass surface was deposited by electrochemically in a monomer-free electrolyte



Scheme 2. Synthetic route for the synthesis of SNS-PDI.

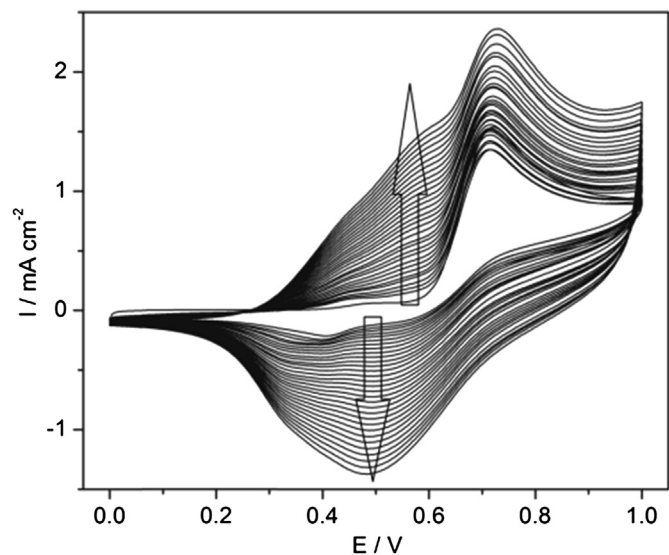


Fig. 1. Repeated potential scanning of SNS-PDI with a scan rate of  $100 \text{ mV s}^{-1}$ , vs. Ag wire.

solution and washed with acetonitrile to remove the oligomeric by-products and residues.

### 3.2. Electrochemical properties

The electrochemical properties of SNS-PDI monomers and corresponding polymers were investigated by cyclic voltammetry (CV) (Fig. 2). During the cathodic scan regime, a cyclic voltammogram of **5** which is referred as PDI standard undergoes two reversible redox couples at  $-0.58$  to  $-0.64 \text{ V}$  ( $E_{r,1/2}^{\text{red}1} = -0.61 \text{ V}$ ) and  $-0.78$  to  $-0.84 \text{ V}$  ( $E_{r,1/2}^{\text{red}2} = -0.81 \text{ V}$ ) which are attributed to two-electron stepwise reduction processes of PDI moiety (Fig. 2a) [42]. In comparison to PDI standard, SNS-PDI has higher electron density on the PDI part because of the electron donating effect of the SNS moiety to PDI. Therefore, the reduction waves of SNS-PDI was observed at more negative regime than that of PDI standard with half wave potentials of  $E_{m,1/2}^{\text{red}1} = -0.72 \text{ V}$  and  $E_{m,1/2}^{\text{red}2} = -0.91 \text{ V}$  (Fig. 2b). In the anodic regime, SNS-PDI exhibited a semi-reversible oxidation wave with

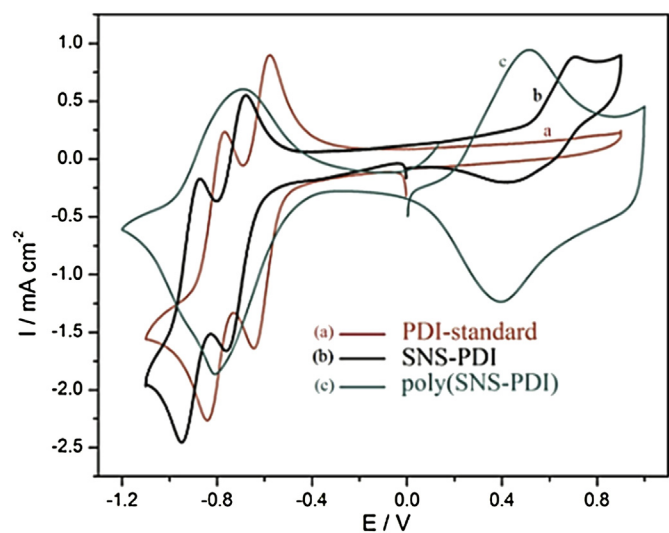


Fig. 2. Cyclic voltammograms of (a) PDI standard (b) SNS-PDI (c) poly-SNS-PDI in TBAPF<sub>6</sub>/CH<sub>2</sub>Cl<sub>2</sub> with a scan rate of  $100 \text{ mV s}^{-1}$ , vs. Ag wire.

half wave potential ( $E_{m,1/2}^{\text{ox}}$ ) of  $0.57 \text{ V}$  observed as a result of attached SNS unit on the PDI-acceptor core (Fig. 2b). This positive shift of the potential proved that there is a slight interaction between PDI and SNS at the neutral state, though there is no conjugation between them. Upon the electrochemical polymerization, polymer deposited onto WE was immersed into the monomer-free electrolyte for CV measurement to determine the oxidation and the reduction potentials. At the end of the electrochemical polymerization, the semi-reversible oxidation became reversible, broader and shifted to lower potential with half wave potential of ( $E_{p,1/2}^{\text{ox}}$ )  $0.45 \text{ V}$  (Fig. 2c) due to extended conjugation on the backbone of SNS-donor. Beside these, the reversible two step reduction became broader and shifted positively to half wave potential of  $E_{p,1/2}^{\text{red}1} = -0.75 \text{ V}$  (Fig. 2c). These results indicated that a donor-acceptor polymer working as both anodically and cathodically in a narrow potential range was obtained. Also, by using oxidation and reduction onsets, the electrochemical band gaps for SNS-PDI monomer and corresponding polymer were calculated as  $1.13 \text{ eV}$  and  $0.72 \text{ eV}$ , respectively. The dramatic decrease in the band gap of the corresponding polymer results from enlargement of  $\pi$ - $\pi$  conjugation of SNS-donor moiety.

### 3.3. Optical properties

The optical properties of the SNS-PDI donor-acceptor system were investigated by UV-Vis absorption and fluorescence spectroscopy recorded with a concentration of  $2 \times 10^{-6} \text{ M}$  solution in CH<sub>2</sub>Cl<sub>2</sub> (Fig. 3). In the UV-Vis spectra of standard PDI, characteristic triple bands of PDI at  $455$ ,  $487$  and  $522 \text{ nm}$  were observed (Fig. 3a) [29]. After attaching SNS moiety, no change in PDI absorption bands was observed, however a new band at about  $328 \text{ nm}$  arising from SNS unit appeared (Fig. 3b). This result provides an evidence for the lack of electronic interaction between SNS-donor and PDI-acceptor in the ground state. In the fluorescence spectrum of PDI standard, characteristic triple bands of PDI at  $541$ ,  $580$ ,  $616 \text{ nm}$  was observed using excitation at  $487 \text{ nm}$  (Fig. 3a) [29]. However, when the fluorescence spectra of SNS-PDI was examined, a remarkable fluorescence quenching was noted almost in the same spectral region of the PDI excited at  $487 \text{ nm}$  where emission of SNS moiety is at minimum (Fig. 3b). This indicates that there is an intra-molecular charge transfer from SNS-donor to PDI-acceptor at the excited state [37,43,44]. Furthermore, the energy transfer process in the molecule was studied by fluorescence spectroscopy of the SNS-PDI. We investigated the fluorescence spectrum using excitation at  $328 \text{ nm}$ , since at this wavelength SNS has a strong absorption where the emission of PDI is at a minimum. The fluorescence of both SNS moiety and PDI in the molecule is quenched strongly, indicating a very efficient deactivation of its excited state. We believe that simultaneous energy and electron transfer processes from SNS to PDI results in the fluorescence quenching of not only the SNS moiety but also PDI in the molecule. Fluorescence quenching experiments using PDI as fluorophore and SNS as quencher were conducted. The results showed that as SNS-standard concentration increases, the emission intensity of PDI standard decreases (is quenched) when excited at both  $328 \text{ nm}$  and  $487 \text{ nm}$  which confirms that the quenching is mainly via electron transfer mechanism (see Supplementary data Fig. S10–12). Overall, photophysical studies exhibited that high efficiencies of both electron and energy transfer from SNS-donor to PDI-acceptor [44,45].

Upon comparison of the optical and electrochemical band gaps (Table 1), these values are not in a good agreement. It shows that the photoactive centers and electroactive centers behave independent from each other.

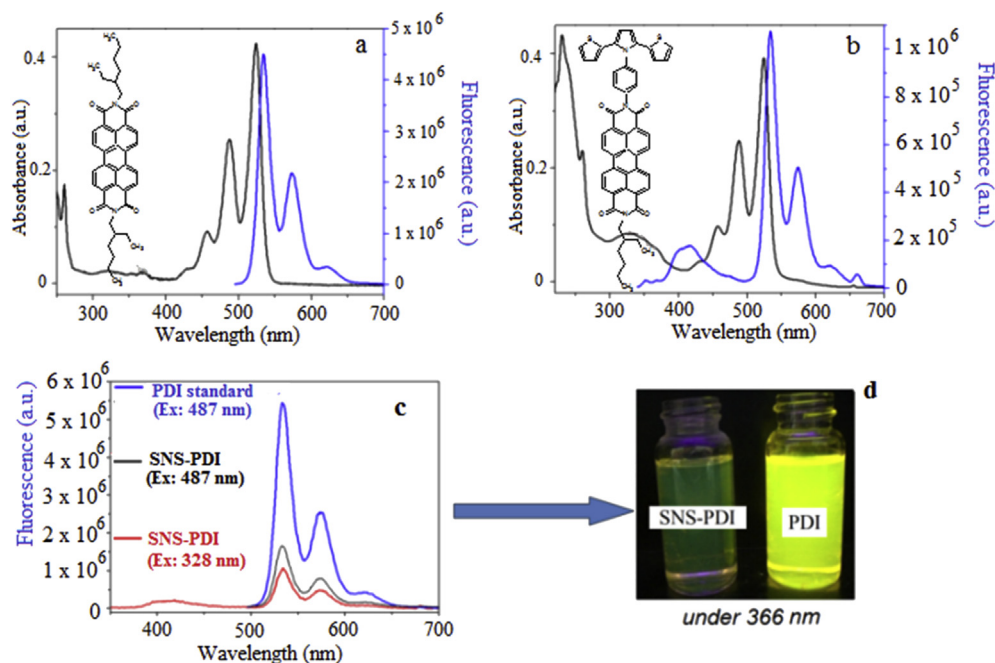


**Fig. 3.** UV–Vis absorption and fluorescence spectra of **PDI** standard (a), **SNS-PDI** (b), and comparison of fluorescence intensity (c) and fluorescence quenching (d) in dichloro-methane solution.

In addition, frontier molecular orbitals have been studied by DFT calculations with Spartan10 program at the parameters of B3LYP and 6-31G\*\* basis set. The charge distribution in the frontier molecular orbitals is shown in Fig. 4. These calculations support the efficient charge separation between SNS-donor and PDI-acceptor obtained data from electrochemical and optical measurements. As expected, the HOMO of SNS-PDI is localized completely on the SNS-donor part, while the LUMO completely exists on the PDI-acceptor part. The charge separations at HOMO and LUMO energy levels confirm that there is no interaction between SNS-donor and PDI-acceptor at the neutral state.

### 3.4. Spectro-electrochemical properties

Optical behavior of poly-SNS-PDI film deposited onto ITO/glass surface against to p- and n-doping processes were studied intensively. The dominant red color of PDI part is used to determine the color of neutral state of SNS-PDI and poly-SNS-PDI. Upon applied

positive potential to poly-SNS-PDI film, the valance-conduction band between 400 and 600 nm (blue to green regime) show no remarkable change between 0.0 and 1.0 V (Fig. 5). In the anodic scan regime of SNS-PDI, the intensified broad band at about 900 nm indicated the formation of polarons and bipolarons on SNS moiety of polymer backbone. As a result of applied positive potential of 0–1.0 V to the polymer, the red colored film (L: 34; a: 51; b: 46) turned into khaki (L: 33; a: –19; b: –2) and then dark blue (L: 13; a: 19; b: –35), respectively.

On the other hand, mono-anion and di-anion radicals formed on the carbonyl groups of the PDI moiety of the poly-SNS-PDI structure in the negative regime. Upon applied potential between 0 and –0.9 V, new absorption bands attributed to mono-anion radicalic form of poly-SNS-PDI intensified at 704, 802, and 960 nm (Fig. 6). Besides, the slight decrease in the intensity of main band of neutral state at about 480 nm leads to color conversion from red (L: 34; a: 51; b: 46) to violet (L: 24; a: 20; b: –31).

**Table 1**

HOMO and LUMO energy levels, electrochemical ( $E'_g$ ) and optical band gaps ( $E_g$ ) of SNS-PDI and poly-SNS-PDI.

Molecule	Reduction peak potentials (V)	Oxidation peak potentials (V)	HOMO (eV)	LUMO (eV)	$E'_g$ , electrochemical band gap (eV)	$E_g$ , optical band gap (eV)
	PDI (C=O)	SNS (ring)				
SNS-PDI	$E_{m,c}^{red1} = -0.76$	$E_{m,a}^{ox1} = 0.70$	–4.95	–3.82	1.13	2.32
	$E_{m,a}^{red1} = -0.68$	$E_{m,c}^{ox1} = 0.43$				
	$E_{p,c}^{red2} = -0.95$	<i>semi-reversible</i>				
	$E_{m,a}^{red2} = -0.87$	$E_{m,on}^{ox} = 0.53$				
	<i>reversible</i>					
Poly (SNS-PDI)	$E_{m,on}^{red} = -0.60$	$E_{p,a}^{ox1} = 0.50$	–4.63	–3.91	0.72	2.20
	$E_{p,c}^{red} = -0.80$	$E_{p,c}^{ox1} = 0.40$				
	$E_{p,a}^{red} = -0.70$	<i>reversible</i>				
	<i>reversible</i>					
	$E_{p,on}^{red} = -0.51$	$E_{p,on}^{ox} = 0.21$				

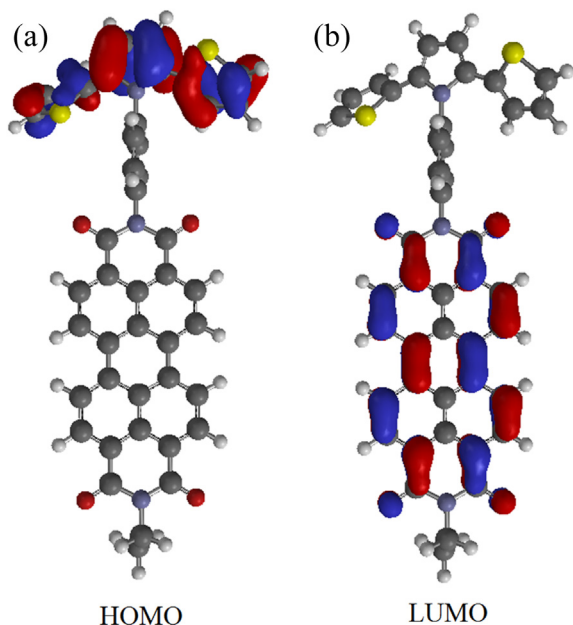


Fig. 4. Molecular orbital diagrams of the a) HOMO and b) LUMO levels of the SNS-PDI.

During the second reduction process of poly-SNS-PDI, the bands attributed to mono-anion form of polymer film disappeared, and the new band intensified at 490, 520 and 575 nm upon applied potential of  $-0.9$  to  $-1.2$  V (Fig. 7). According to this absorption spectrum, violet colored film (L: 24; a: 20; b:  $-31$ ) turned into purple (L: 20; a: 30; b:  $-18$ ).

Overall, poly-SNS-PDI exhibits both reversible oxidation and reduction waves with two redox couples attributed to two-electron stepwise reduction processes of PDI moiety. Considering these properties, poly-SNS-PDI, as an electrochromic material, has furnished multiple separate colors appeared as dianionic, anionic, neutral, polaronic and bipolaronic species at range of only  $-1.2$ – $1.0$  V (Fig. 8). Such a narrow range multi-electrochromism offers a great advantage in various ECDs applications.

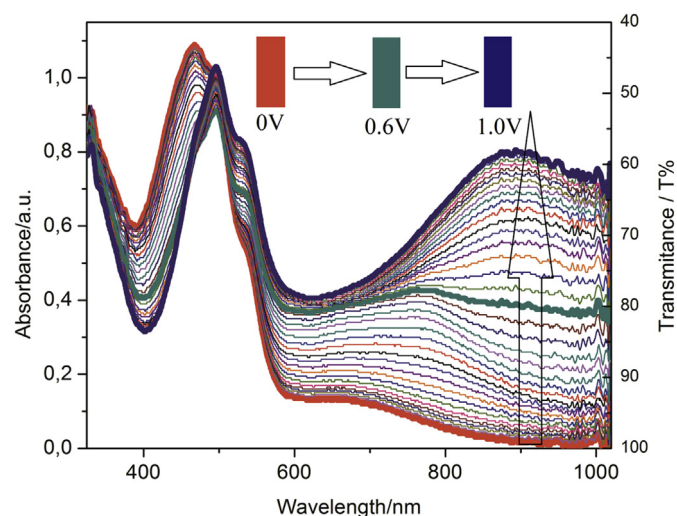


Fig. 5. Spectro-electrochemical measurements and color changes of poly-SNS-PDI film deposited onto ITO/glass surface with applied potential of 0 V–1.0 V.

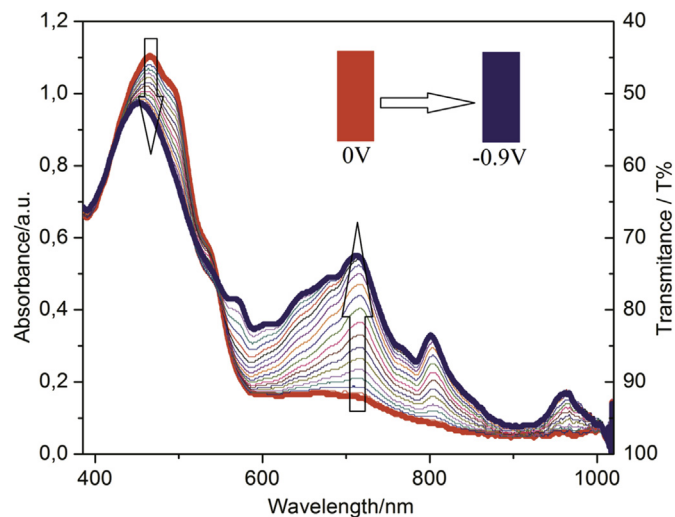


Fig. 6. Spectro-electrochemical measurements and color changes of poly-SNS-PDI film deposited onto ITO/glass surface with applied potential of 0V to  $-0.9$  V.

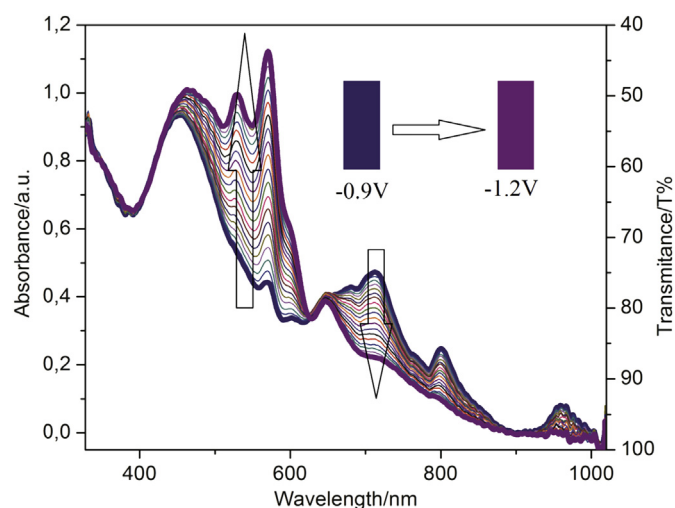


Fig. 7. Spectro-electrochemical measurements and color changes of poly-SNS-PDI film deposited onto ITO/glass surface with applied potential of  $-0.9$  V to  $-1.2$  V.

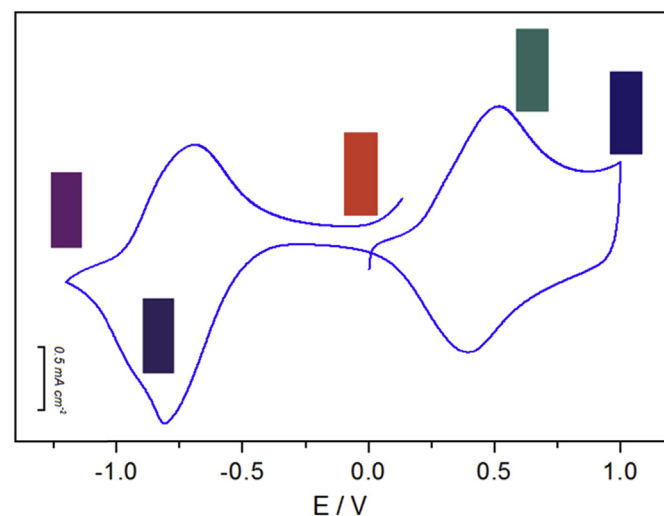


Fig. 8. Color changes of poly-SNS-PDI film deposited onto ITO/glass surface with applied potential of  $-1.2$  V to 1.0 V.

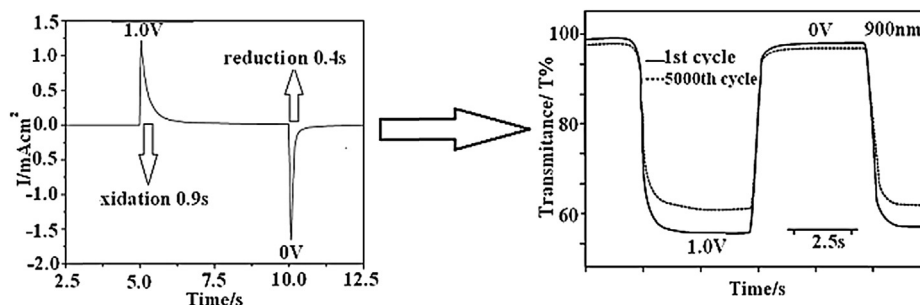


Fig. 9. Chronoabsorptometry experiments for poly-SNS-PDI deposited onto ITO with a switched potential of 0 V–1.0 V.

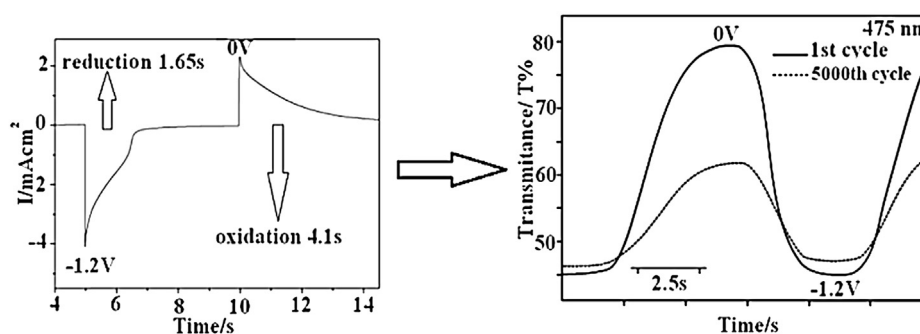


Fig. 10. Chronoabsorptometry experiments for poly-SNS-PDI deposited onto ITO with a switched potential of 0 V to –1.2 V.

Additionally, double step chronoamperometry technique was used to monitor the changes in the electro-optical responses of the SNS-PDI polymer film during anodically and cathodically switching. Electrochromic parameters of the polymer film was analyzed by observing the changes in the transmittance (increments or decrements of the absorption band with respect to time) during stepwise switching the potential between neutral, oxidized and reduced states with a residence time of 5 s. In the anodic regime the change in maximum percentage transmittance ( $\Delta T\%$ ) of poly-SNS-PDI between the neutral (0 V) and oxidized states (1.0 V) were found 48% (Fig. 9). Besides, the oxidation and reduction response times, which is the time required to change a color between a “bleached” state and a “colored state”, or between two colored states, were measured as 0.9 and 0.4 s for poly-SNS-PDI. Optical activities of the poly-SNS-PDI film were retained by 92% even after 5000 cycles of operation (Fig. 9).

However, in the cathodic regime, the change in maximum percentage transmittance ( $\Delta T\%$ ) of poly-SNS-PDI between the neutral (0 V) and reduced states (–1.2 V) were found 34% (Fig. 10). The reduction and oxidation response times were measured as 1.65 and 4.10 s for poly-SNS-PDI. Optical activities of the poly-SNS-PDI film were retained by 46% after 5000 cycles of operation (Fig. 10).

The coloration efficiency (CE) is one of the most important issues for the electrochromic application. CE was calculated by using  $CE = \Delta OD/Q_d$  and  $\Delta OD = \log(T_{\text{colored}}/T_{\text{bleached}})$ , where  $Q_d$  is the injected/ejected charge between neutral and oxidized states,  $T_{\text{colored}}$  and  $T_{\text{bleached}}$  are the transmittance in the oxidized-neutral and/or reduced-neutral states, respectively. In the anodic regime, upon switching potential (deposited onto ITO glass surface with an active area of 1 cm<sup>2</sup>) between 0 V and 1.0 V, CE of poly-SNS-PDI was measured as 254 cm<sup>2</sup> C<sup>-1</sup> by chronoamperometry. On the other hand, CE was measured as 112 cm<sup>2</sup>, with a switched potential between 0 V and –1.2 V. In consequence, the coloration efficiency of poly-SNS-PDI in the anodic regime is one of the highest values for

SNS type electrochromic polymers reported in the literature [26,46–50].

#### 4. Conclusion

Herein, we report the synthesis and characterization of a new electroactive monomer and corresponding polymer consisting of SNS-donor and PDI-acceptor moieties. The monomer SNS-PDI was directly polymerized by electrochemical means onto transparent ITO/glass surface to give electrochromic polymer film. Because of the efficient intramolecular electron transfer from SNS-donor to PDI-acceptor at the excited state, a remarkable fluorescence quenching of the perylene core was observed. Frontier molecular orbitals have been studied by DFT calculations and the charge distributions at HOMO and LUMO confirm the absence of communication between SNS-donor and PDI-acceptor at the neutral state. In addition, electrochromic properties of the polymer films were investigated by the spectro-electrochemical measurements. Poly-SNS-PDI exhibited an ambipolar multi-electrochromic behavior including purple, violet-red-khaki-blue colors in both anodic and cathodic regime in a narrow range of –1.2–1.0 V. Furthermore, electrochemical and electrochromic results such as reversible redox behavior both at anodic and cathodic regime, low response time, high resistance to over oxidation, low driving potential and high coloration efficiency point out that poly-SNS-PDI would be promising material for the construction and/or the development of ECDs and optical displays.

#### Acknowledgment

We gratefully acknowledge the supports from Çanakkale Onsekiz Mart University Grants Commission (Project Number: 2010/99).

## Appendix A. Supplementary data

Supplementary data related to this article can be found at <http://dx.doi.org/10.1016/j.dyepig.2014.08.003>.

## References

- [1] Shirakawa H, Louis EJ, MacDiarmid AG, Chiang CK, Heeger AJ. Synthesis of electrically conducting organic polymers: halogen derivatives of polyacetylene. (CH)<sub>x</sub>. *JCS Chem Comm* 1977;578–80.
- [2] Naarmann H. Synthesis of electrically conducting polymers. *Angew Makromol Chem* 1982 Dec;109:295–338.
- [3] Chen SF, Deng LL, Xie J, Peng L, Xie LH, Fan QL, et al. Recent developments in top-emitting organic light-emitting diodes. *Adv Mater* 2010;22(46):5227–39.
- [4] Lee PI, Hsu SLC, Lin PY. White-light-emitting diodes from single polymer systems based on polyfluorene copolymers with quinoxaline derivatives. *Macromolecules* 2010;43(19):8051–7.
- [5] Kraft A, Grimsdale AC, Holmes AB. Electroluminescent conjugated polymers – seeing polymers in a new light. *Angew Chem Int Ed* 1998;37(4):402–28.
- [6] Grimsdale AC, Chan KL, Martin RE, Jokisz PG, Holmes AB. Synthesis of light-emitting conjugated polymers for applications in electroluminescent devices. *Chem Rev* 2009;109(3):897–1091.
- [7] Horiuchi N, Wenham S. Towards highly efficient solar cells. *Nat Photonics* 2012;6(3):136–7.
- [8] Liu F, Gu Y, Wang C, Zhao Y, Chen D, Briseno AL, et al. Efficient polymer solar cells based on a low bandgap semi-crystalline DPP polymer-PCBM blends. *Adv Mater* 2012;24(29):3947–51.
- [9] Yu G, Gao J, Hummelen JC, Wudl F, Heeger AJ. Polymer photovoltaic cells – enhanced efficiencies via a network of internal donor-acceptor heterojunctions. *Science* 1995;270(5243):1789–91.
- [10] Bronstein H, Chen ZY, Ashraf RS, Zhang WM, Du JP, Durrant JR, et al. Thieno [3,2-b]thiophene-diketopyrrolopyrrole-containing polymers for high-performance organic field-effect transistors and organic photovoltaic devices. *J Am Chem Soc* 2011;133(10):3272–5.
- [11] Morana M, Koers P, Waldauf C, Koppe M, Muehlbacher D, Denk P, et al. Organic field-effect devices as tool to characterize the bipolar transport in polymer-fullerene blends: the case of P3HT-PCBM. *Adv Funct Mater* 2007;17(16):3274–83.
- [12] Mortimer RJ, Dyer AL, Reynolds JR. Electrochromic organic and polymeric materials for display applications. *Displays* 2006;27(1):2–18.
- [13] Baetens R, Jelle BP, Gustavsen A. Properties, requirements and possibilities of smart windows for dynamic daylight and solar energy control in buildings: a state-of-the-art review. *Sol Energy Mater Sol Cells* 2010;94(2):87–105.
- [14] Beaupre S, Breton AC, Dumas J, Leclerc M. Multicolored electrochromic cells based on poly(2,7-carbazole) derivatives for adaptive camouflage. *Chem Mater* 2009;21(8):1504–13.
- [15] Agrawal AK, Jenekhe SA. Synthesis and processing of heterocyclic polymers as electronic, optoelectronic, and nonlinear-optical materials 3. New conjugated polyquinolines with electron-donor or electron-acceptor side groups. *Chem Mater* 1993;5(5):633–40.
- [16] Havinga EE, Tenhoeve W, Wynberg H. Alternate donor-acceptor small-bandgap semiconducting polymers – polysquaraines and polycroconaines. *Synth Met* 1993;55(1):299–306.
- [17] Blanco R, Gomez R, Seoane C, Segura JL, Mena-Osteritz E, Bauerle P. An ambipolar peryleneamide monoimide-fused polythiophene with narrow band gap. *Org Lett* 2007;9(11):2171–4.
- [18] Akoudad S, Roncali J. Electrogenated poly(thiophenes) with extremely narrow bandgap and high stability under n-doping cycling. *Chem Commun* 1998;(19):2081–2.
- [19] Beaujuge PM, Reynolds JR. Color control in pi-conjugated organic polymers for use in electrochromic devices. *Chem Rev* 2010;110(1):268–320.
- [20] Durmus A, Gunbas GE, Camurlu P, Toppare L. A neutral state green polymer with a superior transmissive light blue oxidized state. *Chem Commun* 2007;(31):3246–8.
- [21] Sonmez G, Shen CKF, Rubin Y, Wudl F. A red, green, and blue (RGB) polymeric electrochromic device (PECD): the dawning of the PECD era. *Angew Chem Int Ed* 2004;43(12):1498–502.
- [22] Sonmez G, Sonmez HB. Polymeric electrochromics for data storage. *J Mater Chem* 2006;16(25):2473–7.
- [23] Sonmez G, Sonmez HB, Shen CKF, Wudl F. Red, green, and blue colors in polymeric electrochromics. *Adv Mater* 2004;16(21):1905.
- [24] Sonmez G, Sonmez HB, Shen CKF, Jost RW, Rubin Y, Wudl F. A processable green polymeric electrochromic. *Macromolecules* 2005;38(3):669–75.
- [25] Amb CM, Dyer AL, Reynolds JR. Navigating the color palette of solution-processable electrochromic polymers. *Chem Mater* 2011;23(3):397–415.
- [26] Koyuncu FB, Sefer E, Koyuncu S, Ozdemir E. The new branched multi-electrochromic materials: enhancing the electrochromic performance via longer side alkyl chain. *Macromolecules* 2011;44(21):8407–14.
- [27] Ono K, Totani H, Ohkita M, Saito K, Kato M. Electrochemical polymerization of tetramethylene-crosslinked bis(2,5-di-2-thienyl-1H-pyrrole). *Heterocycles* 2004;64:223–8.
- [28] Just PE, Chane-Ching KI, Lacaze PC. Synthesis of 2,5-di(2-thienyl)-1H-pyrrole N-linked with conjugated bridges. *Tetrahedron* 2002;58(18):3467–72.
- [29] Ahrens MJ, Sinks LE, Rybtchinski B, Liu WH, Jones BA, Giaimo JM, et al. Self-assembly of supramolecular light-harvesting arrays from covalent multichromophore perylene-3,4 : 9,10-bis(dicarboximide) building blocks. *J Am Chem Soc* 2004;126(26):8284–94.
- [30] Schenning APHJ, von Herrikhuyzen J, Jonkheijm P, Chen Z, Wurthner F, Meijer EW. Photoinduced electron transfer in hydrogen-bonded oligo(p-phenylene vinylene)-perylene bisimide chiral assemblies. *J Am Chem Soc* 2002;124(35):10252–3.
- [31] Kaletas BK, Dobrawa R, Sautter A, Wurthner F, Zimine M, De Cola L, et al. Photoinduced electron and energy transfer processes in a bichromophoric pyrene-perylene bisimide system. *J Phys Chem A* 2004;108(11):1900–9.
- [32] Wang HY, Peng B, Wei W. Solar cells based on perylene bisimide derivatives. *Prog Chem* 2008;20(11):1751–60.
- [33] Neuteboom EE, van Hal PA, Janssen RAJ. Donor-acceptor polymers: a conjugated oligo(p-phenylene vinylene) main chain with dangling perylene bisimides. *Chem Eur J* 2004;10(16):3907–18.
- [34] Schweiger LF, Ryder KS, Morris DG, Glidle A, Cooper JM. Strategies towards functionalised electronically conducting organic copolymers. *J Mater Chem* 2000;10(1):107–14.
- [35] Varis S, Ak M, Tanyeli C, Akhmedov IM, Toppare L. Synthesis and characterization of a new soluble conducting polymer and its electrochromic device. *Solid State Sci* 2006;8(12):1477–83.
- [36] Yildiz E, Camurlu P, Tanyeli C, Akhmedov I, Toppare L. A soluble conducting polymer of 4-(2,5-di(thiophen-2-yl)-1H-pyrrol-1-yl)benzenamine and its multichromic copolymer with EDOT. *J Electroanal Chem* 2008;612(2):247–56.
- [37] Koyuncu S, Zafer C, Koyuncu FB, Aydin B, Can M, Sefer E, et al. A new donor-acceptor double-cable carbazole polymer with perylene bisimide pendant group: synthesis, electrochemical, and photovoltaic properties. *J Polym Sci Part A Polym Chem* 2009;47(22):6280–91.
- [38] Yu G, Yang Y, Cao Y, Pei Q, Zhang C, Heeger AJ. Measurement of the energy gap in semiconducting polymers using the light-emitting electrochemical cell. *Chem Phys Lett* 1996;259(3–4):465–8.
- [39] Patil AO, Heeger AJ, Wudl F. Optical-properties of conducting polymers. *Chem Rev* 1988;88(1):183–200.
- [40] Kaim W, Fiedler J. Spectroelectrochemistry: the best of two worlds. *Chem Soc Rev* 2009;38(12):3373–82.
- [41] Mortimer RJ, Reynolds JR. In situ colorimetric and composite coloration efficiency measurements for electrochromic Prussian blue. *J Mater Chem* 2005;15(22):2226–33.
- [42] Lee SK, Zu YB, Herrmann A, Geerts Y, Mullen K, Bard AJ. Electrochemistry, spectroscopy and electrogenerated chemiluminescence of perylene, terrylene, and quaterylene diimides in aprotic solution. *J Am Chem Soc* 1999;121(14):3513–20.
- [43] Zang L, Liu RC, Holman MW, Nguyen KT, Adams DM. A single-molecule probe based on intramolecular electron transfer. *J Am Chem Soc* 2002;124(36):10640–1.
- [44] Korzdorfer T, Tretiak S, Kummel S. Fluorescence quenching in an organic donor-acceptor dyad: a first principles study. *J Chem Phys* 2009;131(3).
- [45] Takahashi M, Morimoto H, Miyake K, Yamashita M, Kawai H, Sei Y, et al. Evaluation of energy transfer in perylene-cored anthracene dendrimers. *Chem Commun* 2006;(29):3084–6.
- [46] Koyuncu S, Usluer O, Can M, Demic S, Icli S, Sariciftci NS. Electrochromic and electroluminescent devices based on a novel branched quasi-dendric fluorene-carbazole-2,5-bis(2-thienyl)-1H-pyrrole system. *J Mater Chem* 2011;21(8):2684–93.
- [47] Koyuncu S, Zafer C, Sefer E, Koyuncu FB, Demic S, Kaya I, et al. A new conducting polymer of 2,5-bis(2-thienyl)-1H-(pyrrole) (SNS) containing carbazole subunit: electrochemical, optical and electrochromic properties. *Synth Met* 2009;159(19–20):2013–21.
- [48] Sefer E, Koyuncu FB, Oguzhan E, Koyuncu S. A new near-infrared switchable electrochromic polymer and its device application. *J Polym Sci Part A Polym Chem* 2010;48(20):4419–27.
- [49] Cihaner A, Algi F. A processable rainbow mimic fluorescent polymer and its unprecedented coloration efficiency in electrochromic device. *Electrochim Acta* 2008;53(5):2574–8.
- [50] Cihaner A, Algi F. Processable electrochromic and fluorescent polymers based on N-substituted thienylpyrrole. *Electrochim Acta* 2008;54(2):665–70.